Sox9 plays multiple roles in the lung epithelium during branching morphogenesis

Briana E. Rockich[a], Steven M. Hrycaj[b], Hung Ping Shih[c], Melinda S. Nagy[b], Michael A. H. Ferguson[b], Janel L. Kopp[c], Maike Sander[c], Deneen M. Wellik[a,b,d], and Jason R. Spence[a,b,d,1]

[a]Department of Cell and Developmental Biology and [b]Department of Internal Medicine, University of Michigan Medical School, Ann Arbor, MI 48109-2200; [c]Department of Pediatrics and Department of Cellular and Molecular Medicine, University of California, San Diego, La Jolla, CA 92093-0651; and [d]Center for Organogenesis, University of Michigan Medical School, Ann Arbor, MI 48109-2200

Edited by Brigid L.M. Hogan, Duke University Medical Center, Durham, NC, and approved October 2, 2013 (received for review June 21, 2013)

Lung branching morphogenesis is a highly orchestrated process that gives rise to the complex network of gas-exchanging units in the adult lung. Intricate regulation of signaling pathways, transcription factors, and epithelial–mesenchymal cross-talk are critical to ensuring branching morphogenesis occurs properly. Here, we describe a role for the transcription factor Sox9 during lung branching morphogenesis. Sox9 is expressed at the distal tips of the branching epithelium in a highly dynamic manner as branching occurs and is down-regulated starting at embryonic day 16.5, concurrent with the onset of terminal differentiation of type 1 and type 2 alveolar cells. Using epithelial-specific genetic loss- and gain-of-function approaches, our results demonstrate that Sox9 controls multiple aspects of lung branching. Fine regulation of Sox9 levels is required to balance proliferation and differentiation of epithelial tip progenitor cells, and loss of Sox9 leads to direct and indirect cellular defects including extracellular matrix defects, cytoskeletal disorganization, and aberrant epithelial movement. Our evidence shows that unlike other endoderm-derived epithelial tissues, such as the intestine, Wnt/β-catenin signaling does not regulate Sox9 expression in the lung. We conclude that Sox9 collectively promotes proper branching morphogenesis by controlling the balance between proliferation and differentiation and regulating the extracellular matrix.

organogenesis | campomelic dysplasia

Lung epithelial morphogenesis is a highly complex and stereotyped process that gives rise to a tree-like network consisting of proximal conducting airways and distal alveoli in which gas exchange occurs in the adult (1–3). In mice, branching morphogenesis begins after the primary lung buds are firmly established and begin to invade into the surrounding mesenchyme at embryonic day 10.5 (E10.5). As the primary lung buds proliferate and continue to invade the surrounding mesenchyme, domain branching initiates (3). The distal tips of the domain branches begin to repetitively bifurcate until terminal saccules form at the canalicular stage (E16.5–E17.5). These saccules will eventually give rise to mature alveoli in the adult mouse (2–5). Several signaling pathways and transcription factors are known to play roles in branching morphogenesis; however, mechanisms controlling morphogenetic movements in the lungs have only recently started to gain attention (1, 6–11).

During branching morphogenesis, the distal tips of the branching epithelium contain a distinct population of progenitor cells that gives rise to all epithelial cell types early in lung development but become developmentally restricted after E16.5 (12, 13). Because this distal epithelium is a highly proliferative population of cells, a fine balance between proliferation and differentiation must be maintained during lung development (14). Several transcription factors are expressed specifically in the distal branching epithelium including Nmyc, Id2, and Sox9 (13-17). Nmyc plays an important role in maintaining the progenitor population in an undifferentiated state and in driving proliferation (14). Lineage tracing experiments have shown that distal tip cells expressing Id2 give rise to both proximal (ciliated, Clara, neuroendocrine cells) and distal (Alveolar type 1 and 2) cell types (13), but a functional role for Id2 in the regulation of lung progenitor cells has not been established. Similarly, Sox9 is expressed in the distal tip epithelium; however, conditional epithelial-specific deletion of Sox9 using surfactant protein C (Sftpc)-driven ablation [SftpC-tetracycline transactivator protein;tetracycline responsive (tetO)-Cre;Sox9-flox] resulted in normal lung development (15). Using an alternative approach [Sonic hedgehog (Shh)-Cre;Sox9-flox], we now report that early and efficient deletion of Sox9 from the lung epithelium results in dramatic defects in branching morphogenesis.

Sox9 is a member of the sex-determining region Y (SRY)-related high mobility group (HMG)-box (SOX) transcription factors family that regulates many developmental processes (18). In humans, mutations in SOX9 can lead to several inherited genetic birth defects, including campomelic dysplasia (CD), acampomelic campomelic dysplasia (ACD), Cooks syndrome, and Pierre Robin sequence (or syndrome) (19–21). Congenital birth defects associated with these disorders can affect many different organ systems, including the respiratory system. Infants that are born with CD/ACD often die in the neonatal period as a result of respiratory distress, which can be a result of abnormal upper airway development or hypoplastic lungs (20–25). In other tissues, Sox9 has a diverse array of functions. For example, pancreatic Sox9 is required for proliferation and branching, intestinal Sox9 acts to limit Wnt-stimulated proliferation, and Sox9 regulates proliferation and extracellular matrix (ECM) production in chondrocytes (26–32). Using genetic gain-of-function (GOF) and loss-of-function (LOF) models, our findings demonstrate that the appropriate level of Sox9 is necessary for

Significance

Human mutations in SOX9 lead to several congenital disorders, including campomelic dysplasia. Babies born with this condition often die of respiratory distress; however, defects in lung development have thus far not been reported in mouse models. Here, we report that epithelial-specific deletion of Sox9 leads to developmental abnormalities in the lung during branching morphogenesis. We demonstrate that Sox9 plays multiple roles in the lung epithelium, balancing proliferation and differentiation and regulating the extracellular matrix. Therefore, our work highlights a role for Sox9 during lung branching morphogenesis, making this a useful model to study defects associated with a congenital disorder affecting humans.

Author contributions: B.E.R., M.A.H.F., D.M.W., and J.R.S. designed research; B.E.R., S.M.H., M.S.N., M.A.H.F., and J.R.S. performed research; H.P.S., J.L.K., and M.S. contributed new reagents/analytic tools; B.E.R., S.M.H., M.S.N., M.A.H.F., D.M.W., and J.R.S. analyzed data; and B.E.R. and J.R.S. wrote the paper.

The authors declare no conflict of interest.

This article is a PNAS Direct Submission.

[1]To whom correspondence should be addressed. E-mail: spencejr@umich.edu.

This article contains supporting information online at www.pnas.org/lookup/suppl/doi:10.1073/pnas.1311847110/-/DCSupplemental.

controlling the number of proliferating cells and differentiating cells, as either loss or gain of Sox9 disrupts this balance. Further, we find dramatic cellular defects when Sox9 is conditionally deleted, which appear to be mediated through both direct and indirect mechanisms. Similar to its role in chondrogenesis, Sox9 transcriptionally regulates ECM genes in the lung epithelium and directly binds to DNA in *Col2a1* regulatory regions. Removing Sox9 leads to a down-regulation of *Col2a1* mRNA and reduced protein expression. We also show that Sox9 leads to defects in laminin deposition, cytoskeletal organization, and cellular movement, although these defects may be indirect. Finally, we show that unlike the intestine (29, 33, 34), Wnt/β-Catenin signaling is not required for Sox9 expression during lung development. Taken together, our results demonstrate that Sox9 plays multiple roles regulating proliferation, differentiation, and the ECM during lung branching morphogenesis.

Results

Epithelial-Specific Loss and Gain of Sox9 Causes Severe Branching Defects in the Lung. Sox9 is expressed in the distal epithelium during branching morphogenesis (E11.5–E16.5) (*SI Appendix*, Fig. S1 *B–E* and ref. 15). After E16.5, Sox9 is down-regulated, terminal differentiation begins, and only a few cells retain Sox9 expression in the late embryonic and postnatal stages. Sox9 is expressed in a manner similar to other distal tip progenitor markers including Nmyc and Id2 (13–15). Previous reports have suggested that epithelial Sox9 is not required for normal lung development (15). We generated lung epithelial conditional LOF (Sox9-floxed) (35) and GOF (Rosa26-tetO-Sox9-mCherry; *Methods*) embryos, using a well-characterized Shh-Cre driver (36). Shh-Cre shows robust activity in the lung epithelium by E10.5 (*SI Appendix*, Fig. S1*A* and ref. 1–3 and 37). Shh-Cre;Sox9-flox/flox lungs (herein referred to as $Sox9^{LOF}$) and Shh-Cre; Rosa-Lox-Stop-Lox-rtTa;Rosa-tetO-Sox9-mCherry lungs (herein referred to as $Sox9^{GOF}$) both develop large, cyst-like structures at the distal epithelial branch tips at all developmental times examined (Fig. 1 *A* and *C* and *SI Appendix*, Fig. S2*A*). Quantitative analysis of branching of in vitro cultured lungs showed a significant reduction in branching in $Sox9^{LOF}$ lungs compared with controls at the start of culture E12.5 (0 h) and after 72 h in culture [0 h: 19.9 ± 1.7 vs. 11.3 ± 1.5 ($P < 0.05$; $n = 3$); 72 h: 57.6 ± 5.9 vs. 38.0 ± 1.7 ($P < 0.05$; $n = 5$)] (Fig. 1*B* and *SI Appendix*, Fig. S2*B*). We confirmed that Sox9 was deleted or overexpressed in the lung epithelium of the respective models with immunochemistry and quantitative (q)RT-PCR (Fig. 1*D* and *SI Appendix*, Fig. S2 *C* and *D*). Cross sections revealed that these cyst-like structures were the result of larger and rounder branch tips compared with control (Fig. 1*E*), which led to large open spaces in $Sox9^{LOF}$ lungs (Fig. 1*F*). We observed a reduction in airway spaces in $Sox9^{GOF}$ at E18.5 (Fig. 1*F*), likely as a result of reduced proliferation in cells expressing ectopic Sox9 (see Fig. 2 and *Discussion*). By E14.5, $Sox9^{LOF}$ and $Sox9^{GOF}$ lungs were noticeably smaller than control lungs (Fig. 1*C* and *SI Appendix*, Fig. S2*F*). This reduction in size was more apparent by E16.5 (*SI Appendix*, Fig. S2*E*); however, all lungs formed the appropriate number of lobes compared with control (*SI Appendix*, Fig. S2*F*).

Ultimately, loss or gain of Sox9 had severe consequences on the health and survival of mice. Of two litters of mice born (to generate $Sox9^{LOF}$), there were five wild-type, five heterozygous, and three $Sox9^{LOF}$ pups. Of the three $Sox9^{LOF}$ pups, one died at birth and two others were euthanized at postnatal day 7 (P7) because of poor health and an apparent difficulty breathing. One litter was born to generate $Sox9^{GOF}$ pups (Sftpc-rtTa;tetO-Sox9-mCherry, Dox started at E15.5). Of six mice, three pups were controls (Sftpc-rtTa or tetO-Sox9-mCherry) that were healthy and thrived at P0 and three were $Sox9^{GOF}$, all of which died at birth. Analysis of the $Sox9^{GOF}$ lungs is discussed here and presented in *SI Appendix*, Fig. S7. Taken together, our data suggest that Sox9 has a previously unappreciated role in regulating branching morphogenesis.

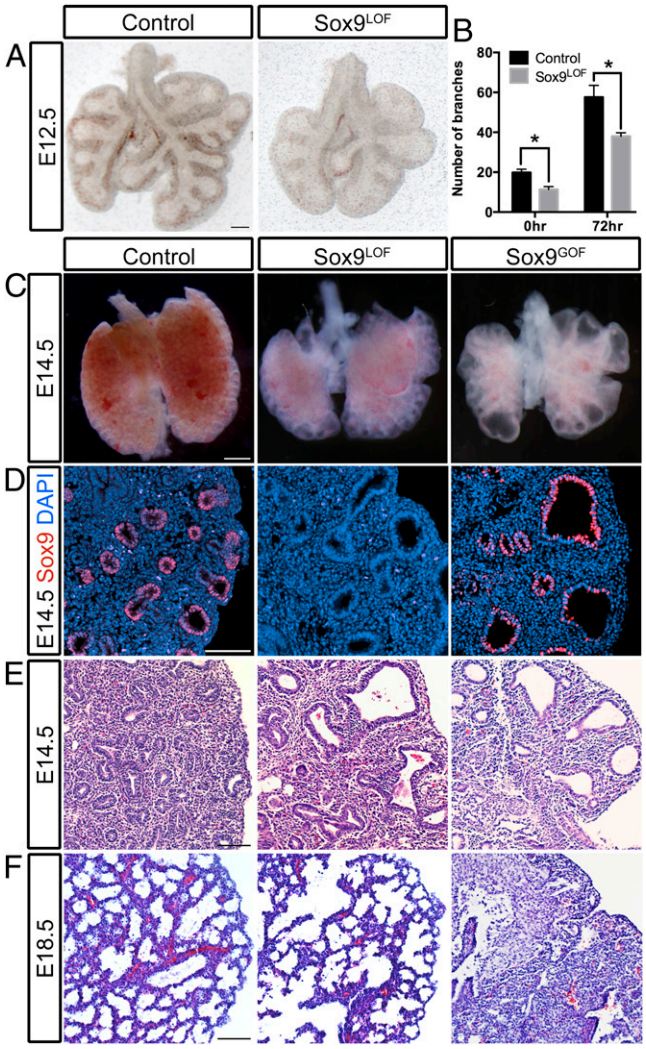

Fig. 1. Sox9 is critical for proper branching morphogenesis. (*A*) Whole-mount images of control and $Sox9^{LOF}$ lungs demonstrate that loss of Sox9 results in fewer domain branches with terminal cystic structures. (*B*) The number of branches was quantified on E12.5 explant lung cultures immediately after dissection (0 h) and after 72 h in culture. $Sox9^{LOF}$ lungs had significantly fewer branches at both times. (*C*) Whole-mount lungs from E14.5 $Sox9^{LOF}$ and $Sox9^{GOF}$ embryos had cystic structures at the distal epithelial tips rather than smaller bifurcations seen in the control lungs. (*D*) Sox9 expression (red) in control, $Sox9^{LOF}$, and $Sox9^{GOF}$ lungs at E14.5. Control lungs had Sox9 expression in the distal epithelial tips. Epithelial Sox9 protein was undetectable in $Sox9^{LOF}$ lungs. $Sox9^{GOF}$ lungs demonstrated robust Sox9 expression in the distal epithelium and ectopic Sox9 expression in the proximal airways. (*E*) H&E staining on sections of E14.5 control, $Sox9^{LOF}$, and $Sox9^{GOF}$ lungs. Staining showed fewer large, cystic buds rather than numerous small buds seen in control lungs. (*F*) H&E staining at E18.5 demonstrates that epithelial cysts led to larger airspaces in $Sox9^{LOF}$ lungs compared with controls. Cystic buds in $Sox9^{GOF}$ lungs appear to have collapsed by E18.5. [(*A* and *C*) Scale bars, 200 μm. (*D–F*) Scale bars, 100 μm.] *$P < 0.05$. Error bars represent SEM.

Precise Regulation of Sox9 Levels Are Required for Appropriate Proliferation in Lung Epithelium. Recent quantitative and live imaging studies have shown that the process of lung bud bifurcation is dynamic and can be separated into three main stages: bud, flattened, and cleft (3, 38). Immunofluorescent staining of Sox9 revealed a dynamic expression pattern during these different stages. Sox9 is expressed highest at the distalmost cells of the

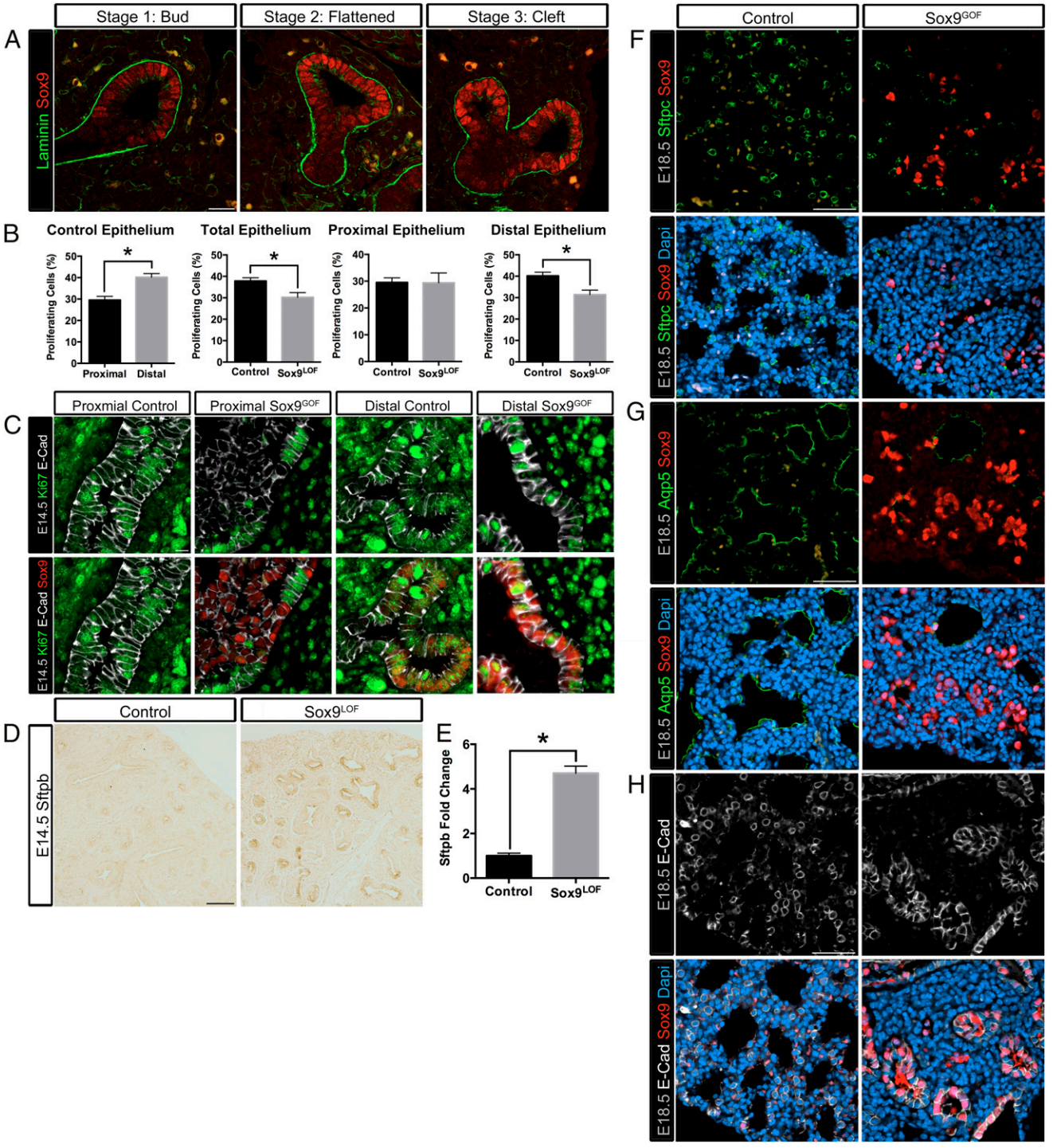

Fig. 2. Sox9 is required for proper proliferation and differentiation of the lung epithelium during branching morphogenesis. (*A*) Sox9 is dynamically expressed during branch bifurcation. Sox9 (red) is expressed highest at the budding tip in stage 1 and the newly formed budding tips in stage 2 and 3. Sox9 expression dissipates toward the parent branch in all three stages and toward the cleft in stage 3. Laminin staining (green) is less robust at the budding tip and most stable at the parent branch and cleft. (*B*) Proliferation in control and $Sox9^{LOF}$ lung epithelium at E14.5 was assessed by BrdU incorporation. In control epithelium, proliferation is significantly higher in distal compared with proximal epithelium ("Control Epithelium"). There is significantly less proliferation in total $Sox9^{LOF}$ epithelium compared with controls ("Total Epithelium"). Comparing proliferation in proximal or distal epithelium of controls vs. $Sox9^{LOF}$ lung epithelium demonstrated that proximal proliferation did not change ("Proximal Epithelium"), whereas a significant reduction in distal epithelial proliferation was seen in $Sox9^{LOF}$ lungs ("Distal Epithelium"). (*C*) Proliferation in control and $Sox9^{GOF}$ lung epithelium at E14.5 was assessed by Ki67 staining. Compared with controls, a dramatic decrease in Ki67 staining (green) was seen in both proximal and distal epithelium (Ecad, white) of $Sox9^{GOF}$ lungs, specifically in cells overexpressing Sox9. (*D* and *E*) Sox9 inhibits differentiation. Sftpb protein is below detection, using immunostaining in control epithelium at E14.5, but was readily detected in $Sox9^{LOF}$ lungs E14.5. qRT-PCR confirmed a greater than fourfold increase in Sftpb mRNA in $Sox9^{LOF}$ lungs compared with controls at E14.5. (*F* and *G*) In E18.5 $Sox9^{GOF}$ lungs, ectopic Sox9 (red) leads to a reduction in Sftpc staining (*F*, green) and Aqp5 (*G*, green) staining. (*H*) Ecad staining (white) revealed that distal $Sox9^{GOF}$ epithelium (red) fails to undergo the columnar-to-squamous epithelial transition seen in lower airways of control lungs. [(*A*) Scale bar, 20 μm. (*C* and *F*) Scale bars, 10 μm. (*D*) Scale bar, 100 μm. (*F–H*) Scale bars, 50 μm.] $*P < 0.01$. Error bars represent SEM.

budding tip and dissipates toward the parent branch (Fig. 2*A*). During the flat and cleft stages, Sox9 is expressed highest where the two new buds will form and lowest where the cleft forms (Fig. 2*A*). Because of the dynamic expression of Sox9 in actively branching buds and previous reports demonstrating increased proliferation in distal lung epithelium (2–5, 14), we wanted to determine whether proliferation was affected in $Sox9^{LOF}$ and $Sox9^{GOF}$ lungs compared with controls. To quantitate proximal and distal proliferation, control or $Sox9^{LOF}$ lungs were costained with Sox2 (proximal epithelium), E-cadherin (Ecad; total epithelium), BrdU (proliferation), and DAPI (total nuclei) (*SI Appendix*, Fig. S3). After a 30-min pulse of BrdU, we determined the percentage of proximal (Ecad+, Sox2+) and distal (Ecad+, Sox2−) proliferation in the epithelium of control and $Sox9^{LOF}$ lungs at E14.5. As previously demonstrated (1, 6–11, 14), we confirmed that distal epithelial proliferation was significantly higher than proximal epithelial proliferation in control tissue (40.2% ± 1.7% vs. 29.6% ± 1.7%; $P < 0.0005$; $n = 12$) (Fig. 2*B* and *SI Appendix*, Fig. S3). Comparing BrdU incorporation in control and $Sox9^{LOF}$ lungs, we found a significant decrease in total epithelial proliferation (37.8% ± 1.5 vs. 30.2% ± 2.2%; $P < 0.01$; $n = 12$), which was a result of reduced proliferation in the distal tip epithelium (40.2% ± 1.7% vs. 31.3% ± 2.1%; $P < 0.005$; $n = 12$), as there was no change in proliferation of the proximal (Sox2+) epithelium when comparing control and $Sox9^{LOF}$ lungs (29.5% ± 1.7% vs. 29.4% ± 3.7%; $n = 12$) (Fig. 2*B* and *SI Appendix*, Fig. S3). There was no change in mesenchymal proliferation between groups (*SI Appendix*, Fig. S3). $Sox9^{GOF}$ lungs had a more dramatic change in proliferation. In the proximal airways of $Sox9^{GOF}$ lungs, cells ectopically expressing Sox9 had almost no Ki67 staining, whereas Ki67 was present in most cells of the control proximal epithelium (Fig. 2*C*). Similarly, cells highly overexpressing Sox9 in the distal epithelium resulted in weak Ki67 staining (Fig. 2*C*). These data suggest that a fine balance of Sox9 expression is necessary to regulate proper proliferation during branching morphogenesis.

To determine whether the perturbations in branching and proliferation in $Sox9^{LOF}$ or $Sox9^{GOF}$ lungs were a result of disruption of well-characterized signaling pathways that regulate lung development, we examined Wnt, Hh, Fgf, and Bmp signaling (2, 12, 13). Using in situ hybridization and/or qRT-PCR in $Sox9^{LOF}$ and $Sox9^{GOF}$ lungs at E12.5 and/or E14.5, we examined key signaling components and target genes and found no significant changes compared with control lungs (*SI Appendix*, Fig. S4 *A* and *B*). In addition, our data demonstrate that proximal–distal patterning is not disrupted in $Sox9^{LOF}$ lungs. In situ hybridization demonstrates that *Bmp4* expression is localized to distal epithelial tips in control and $Sox9^{LOF}$ lungs (*SI Appendix*, Fig. S4*B*) (14, 39, 40), and proximal Sox2 immunostaining is not changed in $Sox9^{LOF}$ lungs compared with controls (*SI Appendix*, Fig. S3). Together, our results suggest that loss of Sox9 regulates proliferation without significantly affecting proximal–distal patterning or the major signaling pathways (Wnt, Fgf, Bmp, Hh) known to play a role in lung branching morphogenesis.

Sox9 Inhibits Differentiation in Early Lung Epithelium. Sox9 is expressed in the distal progenitor population, which gives rise to all cell types of the lung, and Sox9 expression is down-regulated concomitant with onset of cytodifferentiation in the distal epithelium (13–17). In addition, we observed a significant decrease in *Id2* mRNA expression in $Sox9^{LOF}$ lungs at E14.5 by qRT-PCR (*SI Appendix*, Fig. S4*C*). These results, combined with the observed decrease in proliferation in $Sox9^{LOF}$ lungs, led us to hypothesize that Sox9 prevents differentiation of distal progenitors. Differentiation occurs in a proximal-to-distal direction, starting at E14.5 with the differentiation of proximal airway cell types and ending with alveolar type 1 and 2 cell differentiation at E17.5 in the distal airways (2, 15). We examined markers for both proximal and distal epithelial cell types with qRT-PCR and immunostaining. Appropriate temporal differentiation of proximal cell types (Clara and Ciliated cells) and distal type 1 cells occurred in $Sox9^{LOF}$ lungs (*SI Appendix*, Figs. S5 and S6). Sftpc is typically associated with type 2 alveolar cells. However, Sftpc in the early lung marks all distal tip progenitor cells, and recent studies have demonstrated that Sftpc-positive cells in the adult are alveolar stem cells (41). Given that Sftpc can mark progenitor cells, alveolar stem cells, and type 2 differentiated cells, we used surfactant protein B (Sftpb) as a type 2 alveolar cell marker, as it is normally expressed starting at E17.5 (18, 42, 43). In controls, we observed that Sftpb protein was close to background at E14.5 by immunostaining, whereas Sftpb staining in $Sox9^{LOF}$ lungs was readily detectable at this time (Fig. 2*D*). These results were supported by qRT-PCR, which showed a significant increase in *Sftpb* mRNA levels in E14.5 $Sox9^{LOF}$ lungs (Fig. 2*E*), providing evidence that the loss of Sox9 causes precocious differentiation of type 2 cells. In contrast, $Sox9^{GOF}$ lungs demonstrated evidence that terminal differentiation was inhibited. When Sox9 is overexpressed throughout the lung epithelium (Shh-Cre, doxycycline administered starting at E9.5; Fig. 2 *F* and *G* and *SI Appendix*, Figs. S5 and S6) or ectopically expressed in the distal lung epithelium (Sftpc-rtTa, doxycycline administered starting at E15.5; *SI Appendix*, Fig. S7), and lungs were analyzed at E18.5 or P0, respectively, there was decreased expression of proximal and distal differentiation markers (Fig. 2 *F* and *G* and *SI Appendix*, Figs. S5–S7). It is important to point out that differentiated cells observed in $Sox9^{GOF}$ lungs were always Sox9-negative, indicating that they escaped transgene expression, whereas Sox9-positive cells did not express differentiation markers. During terminal differentiation, starting around E17.5, the distal epithelium undergoes a columnar-to-squamous epithelial transition, giving rise to alveolar sacs composed of type 1 and type 2 alveolar cells. Accordingly, air spaces in control lungs at E18.5 were lined by a squamous epithelium; however, the distal epithelium of $Sox9^{GOF}$ lungs remains columnar (Fig. 2*H*). Collectively, our results suggest that Sox9 activity maintains the undifferentiated status of distal lung progenitors. Removing Sox9 leads to early differentiation, and increasing Sox9 prevents differentiation and inhibits the epithelial transition from columnar to squamous epithelium that allows the adult alveoli to form.

Loss of Sox9 Leads to Multiple Cellular Defects in the Distal Progenitor Cells. Because perturbations of epithelial Sox9 led to branching defects and cystic terminal branches, we wanted to detail the cellular events associated with the cystic structures observed in mutant mice. To examine possible cellular defects, we performed transmission electron microscopy in control and $Sox9^{LOF}$ lungs and observed striking disruptions in the $Sox9^{LOF}$ lungs. Whereas the distal epithelial tips of control lungs showed a relatively uniform apical surface with microvilli, apical tight junctions, and a flat, uniform basal surface (Fig. 3*A*), $Sox9^{LOF}$ lungs had a range of defects with varying levels of severity (Fig. 3*B*). $Sox9^{LOF}$ lungs showed defects on the apical surface of the cell. Although tight junctions were observed, apical membranous blebs protruded into the lumen. In some cases, microvilli were absent, and the apical surface appeared rounded and smooth (Fig. 3*B*, lower). Cell–cell adhesion also appeared to be disrupted in $Sox9^{LOF}$ lungs. Although control epithelial cells were in close apposition with occasional gaps, cell–cell adhesion appeared uniformly disrupted in $Sox9^{LOF}$ lungs, with large gaps filled with pseudopodia between the lateral membranes of neighboring cells (Fig. 3*B*). These pseudopodia are similarly observed in lungs with disrupted Cdc42, which have defective epithelial organization (7). Last, the control epithelium has a relatively flat and uniform basal surface that contacts the lung mesenchyme (Fig. 3*A*). In contrast, the basal epithelial surface in $Sox9^{LOF}$ lungs was not uniform, with many cells having a rounded appearance and with membranous blebs projecting into the subcellular space (Fig. 3*B*). Surprisingly,

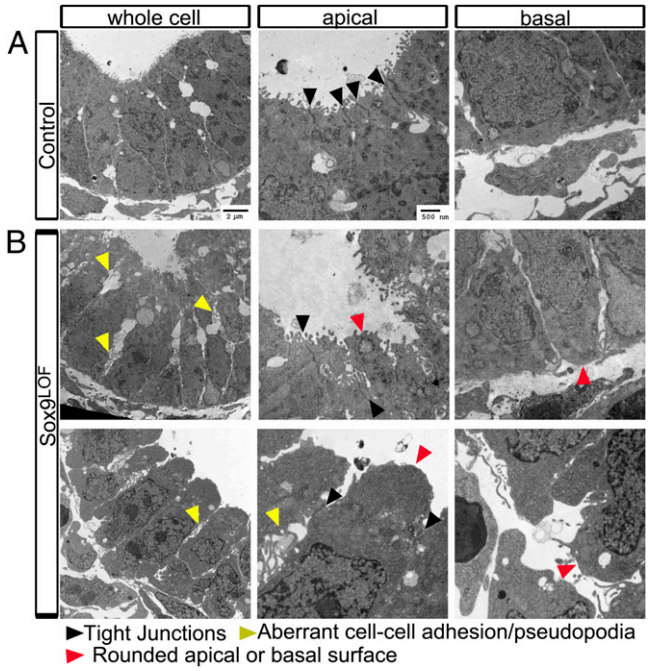

Fig. 3. Cellular defects in Sox9^{LOF} lung epithelium. (*A* and *B*) TEM images of E14.5 control and Sox9^{LOF} lungs revealed intact tight junctions (black arrows). (*B*) Sox9^{LOF} lungs exhibited moderate (*B*, *Middle*) and severe (*B*, *Bottom*) degrees of cellular disruption. This included rounded apical surfaces, loss of microvilli, apical blebbing, and irregular basal surfaces (red arrows). In addition, Sox9^{LOF} lungs had large spaces between adjacent cell membranes that contained pseudopodia (yellow arrows).

the apparent cell adhesion defects we observed by transmission electron microscopy were not obvious when examining E-cad immunofluorescence, although we did note that the epithelium in Sox9^{LOF} lungs was taller than in controls (17.2 μm ± 0.24 μm vs. 15.2 μm ± 0.21 μm; $P < 0.0001$; $n = 192$) (*SI Appendix*, Fig. S8). Given that Sox9 controls multiple cellular processes in different contexts (*Introduction*, *Discussion*), we examined apical–basal polarity and ECM proteins in Sox9^{LOF} and control lungs and found that polarity was unaffected (*SI Appendix*, Fig. S9). However, on examining several proteins that make up and interact with the ECM of the distal lung epithelium (*SI Appendix*, Fig. S9), we found that two proteins (Col2a1 and laminin) were disrupted (Figs. 4 and 5).

Type 2 collagen (Col2a1), which is directly regulated by Sox9 in other contexts and is highly expressed in the distal lung epithelium at E12.5 (44), was significantly reduced in Sox9^{LOF} lungs compared with control (Fig. 4). Immunofluorescence of Col2a1 protein at E12.5 (Fig. 4*A*) and E14.5 (*SI Appendix*, Fig. S10*A*) showed a reduction of staining specifically in distal epithelial buds. This was supported by qRT-PCR on whole lungs at E12.5 and E14.5, which demonstrated significant *Col2a1* down-regulation at both times in Sox9^{LOF} (Fig. 4*B*). To determine whether Sox9 is directly binding *Col2a1* regulatory elements in the distal lung epithelium, we performed Sox9 chromatin immunoprecipitation, using FACS-purified distal lung epithelium from transgenic Sox9-eGFP mice (*SI Appendix*, Fig. S10 *B* and *C*) (45). Using qRT-PCR, we observed that Sox9 was able to bind to a previously characterized consensus binding site located in intron 1 of the *Col2a1* gene with a ~fivefold higher affinity than an IgG control antibody (Fig. 3*C*). In contrast, the same Sox9 antibody did not have increased binding to a nonspecific intergenic region of DNA located near the *Col2a1* intron 1 ("Neg Control" in Fig. 4*C*), whereas an antibody to histone H3 was used as a positive control and bound to both regions of DNA. Collectively, these results are consistent with Sox9 directly regulating *Col2a1* transcription, resulting in proper protein expression.

We also observed defects in laminin deposition in both Sox9^{LOF} and Sox9^{GOF} lungs (Fig. 5 and *SI Appendix*, Fig. S11); however, these effects may be indirect, as we did not detect a transcriptional change in several *Laminin* mRNAs by qRT-PCR (*SI Appendix*, Fig. S11*B*). By examining stage 1 bud tips (Fig. 2*A*), we observed that laminin is deposited by the epithelium as a fine border along the basal side of the epithelial buds in controls (Fig. 2*A* and Fig. 5 *A* and *B*). In contrast, Sox9^{LOF} lungs have a fragmented border around the distal epithelium, with laminin staining being found within the epithelial cell, rather

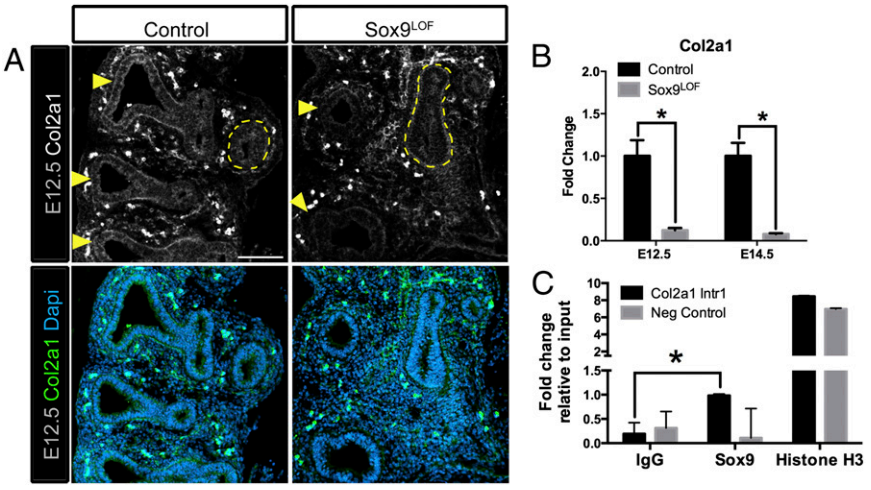

Fig. 4. Sox9 regulates ECM protein Col2a1. (*A*) Col2a1 staining (white, *Upper*; green, *Lower*) was reduced in E12.5 distal buds (yellow arrows) compared with control lungs. Proximal airways are outlined with a yellow dotted line. (*B*) Col2a1 mRNA levels are reduced by an eightfold decrease in E12.5 and a 12-fold decrease in E14.5 lungs compared with control lungs. (*C*) ChIP assay was performed on FACS-purified Sox9-eGFP distal lung epithelial cells. Compared with a nonspecific rabbit anti-IgG, anti-Sox9 preferentially (fivefold enrichment) pulled down a previously characterized Sox9 binding site in Col2a1 intron1 (Col2a1 Intr1, black bars), whereas anti-Sox9 did not pull down nonspecific intergenic DNA near the Col2a1 gene (Neg Control, gray bars). Both Col2a1 Intr1 and nonspecific intergenic DNA (Neg Control) were pulled down with the positive control, anti-Histone H3. All fold changes were normalized to 2% input. (Scale bar, 100 μm.) (*B*) *$P < 0.005$. (*C*) $P < 0.05$. All error bars represent SEM.

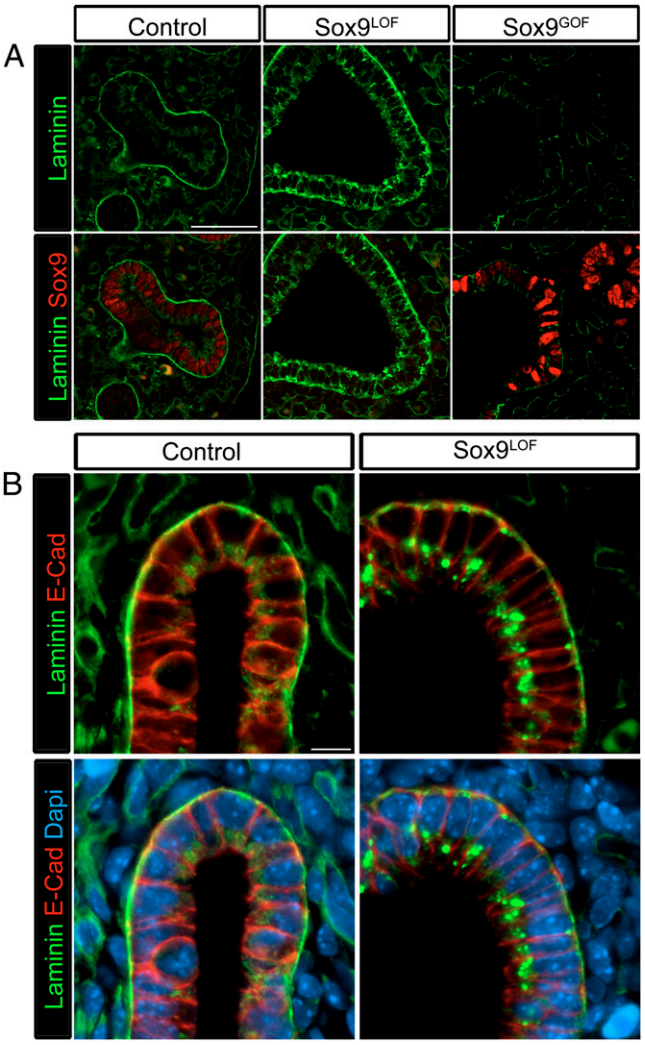

Fig. 5. Gain or loss of Sox9 disrupts basement membrane laminin deposition. (*A*) Laminin staining (green) in control lungs at E14.5 shows robust staining in the basement membrane of Sox9+ (red) branching epithelial tips. In contrast, $Sox9^{LOF}$ lungs showed mislocalized staining, and $Sox9^{GOF}$ had a reduction in laminin staining. (*B*) In $Sox9^{LOF}$ lungs, intracellular laminin staining (green) is observed as punctae on both the apical and basal surfaces of the epithelial (Ecad, red) cells compared with controls, where laminin is part of the ECM of the basement membrane. [(*A*) Scale bars, 50 μm. (*B*) Scale bars, 10 μm.]

than in the basement membrane (Fig. 5 and *SI Appendix*, Figs. S11 and S12). This staining includes large, laminin-positive intracellular punctae observed on the apical and basal surfaces of the cell (Fig. 5 and *SI Appendix*, Figs. S11 and S12). In $Sox9^{LOF}$ lungs, we found that intracellular laminin punctae associate with the Golgi marker gm130 and with the endoplasmic reticulum marker KDELR (*SI Appendix*, Fig. S11 *C* and *D*).

Given the severe cellular disruptions observed by transmission electron microscopy (Fig. 3), we also examined the lung epithelial cytoskeleton, which is important during branching morphogenesis (29, 33, 34, 46, 47). We analyzed the cytoskeleton by using acetylated tubulin (AcTub) and F-actin (Phalloidin) staining (Fig. 6 and *SI Appendix*, Fig. S13). Phalloidin staining is strongest on the apical surface of the cells but is also observed along the basal–lateral surfaces and was not different between control and $Sox9^{LOF}$ lungs (*SI Appendix*, Fig. S13*A*). In contrast, we observed a stark reduction in AcTub staining along the basal surface of the epithelial cells in $Sox9^{LOF}$ lungs (Fig. 6*A*). This indicates that stabilized tubulin is disrupted at the basal surfaces of the epithelial cells in $Sox9^{LOF}$. In $Sox9^{GOF}$ lungs, the cytoskeletal organization was not perturbed compared with control lungs (*SI Appendix*, Fig. S13 *A* and *B*).

Loss of Sox9 Disrupts Epithelial Movement. Because the ECM and microtubule dynamics are strongly associated with cell movement/migration (13–15, 48, 49), and we observed disrupted ECM and stabilized (acetylated) microtubules in $Sox9^{LOF}$ epithelium along the basal surface of the cells, we wanted to determine whether this had an effect on cell movements/migration. As the lung branches, the lung bud grows by coordinating epithelial movement and proliferation (15, 40). Epithelial movement was quantified using an in vitro cell migration scratch assay that has previously been used to assay movement in kidney epithelial buds during branching morphogenesis (35, 50); isolated E12.5 $Sox9^{LOF}$ and control epithelial buds were plated in vitro and exhibited delayed scratch closure compared with controls (Fig. 6 *B* and *C* and *SI Appendix*, Fig. S13). The control epithelial cells migrated 50.1% (±5.3%; $n = 8$ epithelial buds) of the scratch in 3 h and 79.2% (±5.8%; $n = 8$) in 6 h compared with $Sox9^{LOF}$ cells, which only traveled 33.9% (±2.3%; $n = 16$ epithelial buds) in 3 h and 65.5% (±3.7%; $n = 16$) in 6 h ($P < 0.005$ and $P < 0.01$, respectively) (Fig. 6*C* and *SI Appendix*, Fig. S13*C*). Epithelial buds were stained for AcTub, and similar to lung buds in vivo, we observed that stabilized microtubules were disrupted in isolated $Sox9^{LOF}$ buds in vitro, whereas control cells showed uniform organization of the microtubules along the wound edge (Fig. 6*D*).

Sox9 Expression Is Not Regulated by Wnt/β-Catenin in the Lung Epithelium. Because Sox9 is a well-established direct target of β-catenin-dependent Wnt signaling in the intestine (29, 33, 34, 36), and our data show that the Wnt target gene *Axin2* is higher in distal epithelium than proximal epithelium in control lungs by in situ hybridization (*SI Appendix*, Fig. S4*B*), we investigated whether Sox9 is also regulated by Wnt/β-catenin in the developing lung. We generated two Wnt LOF models (β-$Catenin^{LOF}$: $Sox9CreER^{T2}$; β-Catenin-flox/flox lungs and $Lrp5/6^{LOF}$:$Sox9CreER^{T2}$;Lrp5/6-flox/flox) (*SI Appendix*, Fig. S14) (51, 52). In both β-$Catenin^{LOF}$ and $Lrp5/6^{LOF}$ lungs, Sox9 expression is not lost but, rather, expands into the proximal airway, creating a Sox9+/Sox2+ intermediate population of cells that is not seen in control lungs throughout development (*SI Appendix*, Fig. S14). From these results, we conclude that canonical Wnt signaling is not necessary for Sox9 expression in the lung epithelium.

Discussion

A Role for Sox9 in Lung Branching Morphogenesis. In a previous report, deletion of Sox9 in lung epithelium (Sftpc-rtTa;tetO-Cre; Sox9-flox/flox) at E12.5 produced no deleterious developmental consequences in the lung (15). Here, using an earlier and more complete Sox9 deletion (Shh-Cre;Sox9-flox/flox) (E9.5), we document an important role for Sox9 in branching morphogenesis. We observe an obvious branching defect as early as E12.5, along with the complete loss of protein by this time, indicating that Sox9 function is important at the beginning of branching. Importantly, Perl and coworkers also report that Sox4 and Sox11 are present and unchanged in Sox9 mutant lung epithelium at E12.5 and E13.5, suggesting that loss of Sox9 on or after E12.5 may be compensated for by other Sox genes. The strategy we take here and the phenotypes that develop may be highly relevant to the congenital birth defects in CD/ACD, making this an applicable mouse model for the further investigation of those devastating human conditions.

Many signaling pathways and transcription factors are essential for branching morphogenesis. In many cases, when these factors and pathways are perturbed, the consequence is a cystic phenotype, similar to the phenotype seen in both $Sox9^{LOF}$and $Sox9^{GOF}$ lung (7, 10, 14, 53–59). The fact that both gain and loss of Sox9

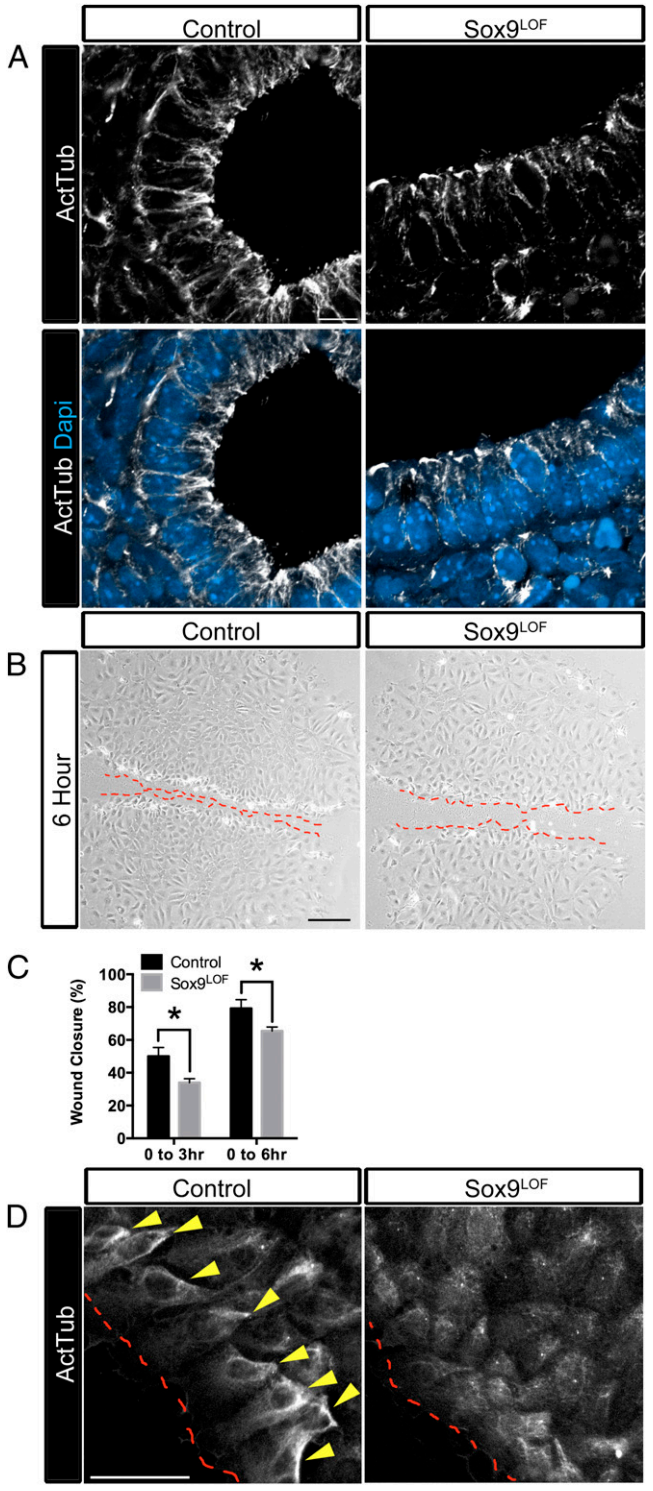

Fig. 6. Sox9 is required for proper cytoskeleton organization and in vitro cellular migration. (*A*) $Sox9^{LOF}$ lungs have a disrupted microtubule cytoskeleton. Stabilized acetylated tubulin (AcTub, white) is observed on the apical, lateral, and basal surfaces of control epithelium at E14.5. In contrast, $Sox9^{LOF}$ epithelium has reduced AcTub staining on the lateral surfaces and no staining along the basal surface of the epithelium. (*B* and *C*) A scratch assay was performed on isolated control and $Sox9^{LOF}$ epithelial buds cultured in vitro to examine epithelial movement characteristics. The red dotted line indicates the scratch. Compared with controls, migration of $Sox9^{LOF}$ epithelial cells was significantly delayed at both 3 and 6 h times, indicating that $Sox9^{LOF}$epithelial cells have impaired cellular migration/movement. Closure of the scratch was quantitated over time (*D*). AcTub staining revealed that in control lungs, the cells lining the scratch had accumulated stabilized tubulin on the side furthest from the scratch (arrows) compared with the $Sox9^{LOF}$ cells, which had no aggregation of ActTub. [(*A*) Scale bar, 50 μm. (*B*) Scale bar, 200 μm. (*C*) Scale bar, 100 μm.] $*P < 0.01$. Error bars represent SEM

resulted in a similar phenotype is likely reflected in the small number of possible outcomes when branching morphogenesis is perturbed; that is, if an epithelial bud cannot properly bifurcate, it gives rise to a larger, cystic sac. We also observed that the E14.5 $Sox9^{GOF}$ cystic phenotype was not present at E18.5 in $Sox9^{GOF}$ lungs (Fig. 1 *E* and *F*). This change in phenotype at E18.5 could be explained by the smaller numbers of cells expressing ectopic Sox9 at this time, likely because cells expressing high levels of ectopic Sox9 had reduced proliferation and a selective disadvantage over developmental time (Fig. 2 *F–H* and *SI Appendix*, Figs. S5 and S6). It is highly possible that cells expressing ectopic Sox9 were outcompeted by normal cells, leading to a partial resolution of the phenotype.

Sox9 Influences ECM and Cell Movement. In addition to proliferation and differentiation, we investigated whether the cystic phenotype resulting from Sox9 perturbations may be a result of abnormal cellular consequences. Studies have shown that Sox9 plays critical roles in both ECM deposition and cell migration in various tissues and diseases (18). In the heart, Sox9 is required for proper organization the valvular ECM proteins (60), whereas in the gonads, Sox9 regulates many ECM proteins as well as modifiers of the ECM such as matrix metalloproteinases (61, 62). Sox9 also plays a role in fibrotic and sclerotic disorders in various tissues, in which Sox9 causes excessive and inappropriate ECM deposition by activating ECM proteins (63–68). Furthermore, Sox9 plays a critical role during chondrogenesis (30), and ChiP analysis in chondrocytes has shown that Sox9 directly binds to loci of 18 different ECM genes, including *Col2a1* (69). Our results support Sox9 as a regulator of ECM in the lung as well, demonstrating that it can transcriptionally regulate *Col2a1* and lead abnormal protein deposition in the basal lamina. We also observed defects in laminin deposition with loss or gain of Sox9 in the branching lung; however, this seems to be an indirect effect of Sox9 perturbations, as we did not observe transcriptional changes in laminin genes. These results also highlight that some of the cellular defects observed in the $Sox9^{LOF}$ or $Sox9^{GOF}$ phenotype may be indirect. Elucidating additional detail as to how perturbations in Sox9 directly and indirectly affect lung epithelial cell morphology and behavior will be an active area of future investigation.

In many contexts, the ECM has a dynamic role associating with and influencing reorganization of the cytoskeleton (70, 71). For example, laminin–integrin-based cell adhesion functions to anchor stabilized microtubule "plus-ends" and maintain the proper microtubule density on the basal surface of epithelial cells (72). Therefore, our results demonstrating disruption of the stabilized microtubule network on the basal side of the lung epithelium in $Sox9^{LOF}$ lungs, and the disorganized microtubule network observed in $Sox9^{LOF}$ distal epithelial cells in the in vitro migration assay, may be explained by perturbations in the ECM. Although the link between Sox9 and cell migration/microtubule organization may be indirect, in other systems Sox9 is critical for cell migration, including neural crest cells during development (73) and tumor metastasis in breast, colon, prostate, and melanoma cancers (74–77). In future studies, it will be pertinent to determine how Sox9 is mechanistically regulating acetylated tubulin and epithelial cell movement during lung branching morphogenesis.

β-Catenin-Dependent Wnt Signaling and Sox9. Sox9 contributes to a diverse range of functions in several endodermally derived organs, including the pancreas, lung, and intestine (26, 27, 78,

79). Wnt signaling is critical for the development of these organ systems, and it has been shown in the developing intestine that Sox9 is a direct target of Wnt signaling (29, 33, 34). Here, we find that in contrast to the intestine, Sox9 transcription in the lung is not regulated by Wnt/β-catenin signaling.

Taken together, our results have established a role for Sox9 during lung branching morphogenesis. We have demonstrated that Sox9 is a multifaceted transcription factor that directly and indirectly regulates proliferation, differentiation, the ECM, cytoskeletal organization, cell shape, and cellular movement.

Methods

Mouse Strains. All mice used in these studies were housed at the University of Michigan mouse facility and were maintained according to the University of Michigan's Committee on Use and Care of Animals (UCUCA)'s protocols. *Shh-Cre*, *Sox9CreER*, *Sox9^{Flox}*, *β-Catenin^{Flox}*, *Rosa-rtTa*, *SftpC-rtTa*, *Lrp5/6^{Flox}*, and *Sox9-eGFP* mice have all been previously described (35, 36, 45, 80–82). Description of the Rosa26-tetO-Sox9 mice is currently under review elsewhere (Philip A. Seymour, Hung Ping Shih, Richard Behringer, Mark Magnuson, and Maike Sander). Briefly, the pTight tetO promoter driving bidirectional expression of Sox9 and mCherry was targeted to the Rosa26 locus. An active rtTa causes transcription of both alleles to be driven independently from the same promoter.

Doxycycline and Tamoxifen Administration. Doxycycline was administered in the drinking water at 2 mg/mL, supplemented with 2.5 mg/mL sucrose started at E9.5 or E15.5 until the time of harvest. Tamoxifen (50 μg/g) was dissolved in corn oil and given via oral gavage once a day for 2 consecutive days (E11.5 and E12.5).

Lung Explant Cultures. Lung explant cultures were performed in vitro, as previously described (83). E12.5 lungs were cultured on Nucleopore polycarbonate track-etch membranes for up to 72 h at 37 °C in a 5% CO_2 incubator. Images of explants were taken on a Leica M125 stereomicroscope. Branches were counted manually.

Migration Scratch Assay. Isolation of epithelial buds from the surrounding mesenchyme of E12.5 lungs was previously described (50). Briefly, lung epithelial buds were placed on BD Matrigel hESC-qualified matrix (BD Biosciences)–coated plates with DMEM/Ham's F-12 supplemented with 50 U/mL penicillin-streptomycin and 0.1% (vol/vol) FBS (Gibco). Epithelial buds grew into colonies by 48 h at 37 °C in a 5% CO_2 incubator. Lung bud cultures were scratched with a micropipette tip, and images were taken on an Olympus SZX16 microscope at 0, 3, and 6 h after the scratch. Scratch width was measured with ImageJ software.

Immunohistochemistry and in Situ Hybridization. Immunostaining was carried out as previously described (84, 85). Antibody information and dilutions can be found in *SI Appendix*, Table S1. All immunofluorescence images were taken on a Nikon A1 confocal microscope. All DAB images were taken on an Olympus IX71 microscope. For section in situ hybridization, embryos were collected in PBS and fixed overnight in 4% paraformaldehyde in PBS (PFA) at 4 °C. Embryos were then rinsed in PBS and immersed in 30% sucrose at 4 °C overnight before embedding into optimal cutting temperature (OCT) media. Frozen sections 12–16 μm in size were cut, and slides were stored at −80 °C. In situ hybridization was performed as previously described (86, 87). *Axin2*, *Bmp4*, and *Shh* in situ probes were previously described (88–90).

qRT-PCR. RNA was extracted from E12.5 or E14.5 lungs, using Purelink RNA Mini Kit (Life Technologies). RNA quantity and quality were determined spectrophotometrically, using a Nano Drop 2000 (Thermoscientific). Reverse transcription was conducted using the SuperScript VILO kit (Invitrogen), according to manufacturer's protocol. Finally, qRT-PCR was carried out using Quantitect Sybr Green MasterMix (Qiagen) on a Step One Plus Real-Time PCR system (Life Technologies). For a list of primer sequences, see *SI Appendix*, Table S2.

Proliferation Quantification. Quantification of BrdU-positive cells that colocalized with Ecad, Sox2, and DAPI was counted with Metamorph cell counting software.

Transmission Electron Microscopy. E14.5 lungs were processed as previously described (91). Using a Philips CM-100 electron microscope, 70-nm sections were imaged.

FACS. E14.5 Sox9-eGFP and control lungs were minced and resuspended in 2 mg/mL Collagenase D (Roche) and 40 U TURBO DNase (Life Technologies) for 2 min. This procedure was then repeated with 2× TrypLE SELECT (Life Technologies) and DNase for 5 min at 37 °C. The cells were gravity filtered through a 70-μm filter. Both Sox9-eGFP and control cells were sorted (*SI Appendix*, Fig. S10)

Chromatin Immunoprecipitation Assay. FACS-sorted distal lung progenitor cells were fixed with 1% (vol/vol) formaldehyde in PBS for 10 min. The reaction was quenched with glycine and washed in 1× PBS. The Cell Signaling SimpleChIP Enzymatic ChIP Kit was used as described by the manufacturer, with the following modification: MNase was not used; rather, nuclei were sonicated (Branson Sonifier 250) 10× for 30-s bursts at 25% duty, output 3.5 with 1 min on ice between bursts.

Cell Length Quantification. The height of the cells was measured from the apical to basal surface of the cell indicated by Ecad stain. Cell height was measured using ImageJ software.

Statistical Analysis. All data are shown as the mean of at least three independent biological replicates; error bars represent SEM. Statistical differences between experimental and control groups were assessed with Prism software, using multiple *t* tests. Results were considered statistically significant at $P < 0.05$.

ACKNOWLEDGMENTS. We thank Dr. Deborah Gumucio for thoughtful comments on the manuscript, Dr. Yukiko Yamashita and Dr. Eric White for helpful experimental input, and Dr. Bart O. Williams for kindly providing the Lrp5 and Lrp6 floxed mice. This work was supported in part by the Bradley M. Patten Student Fellowship (to B.E.R.), a Michigan Institute Clinical Health Research Postdoctoral Translational Scholars Program (MICHR PTSP) fellowship and a National Institutes of Health (NIH) training fellowship (T32 HL 7749-20; to S.M.H.), the University of Michigan Department of Internal Medicine, Biological Sciences Scholars Program, Center for Organogenesis, a March of Dimes Basil O'Connor Research Award (to J.R.S.), and the National Heart, Lung, and Blood Institute (NHLBI) (R01-HL119215; to J.R.S. and D.M.W.).

1. Domyan ET, Sun X (2011) Patterning and plasticity in development of the respiratory lineage. *Dev Dyn* 240(3):477–485.
2. Morrisey EE, Hogan BLM (2010) Preparing for the first breath: Genetic and cellular mechanisms in lung development. *Dev Cell* 18(1):8–23.
3. Metzger RJ, Klein OD, Martin GR, Krasnow MA (2008) The branching programme of mouse lung development. *Nature* 453(7196):745–750.
4. Rawlins EL (2011) The building blocks of mammalian lung development. *Dev Dyn* 240(3):463–476.
5. Warburton D, et al. (2005) Molecular mechanisms of early lung specification and branching morphogenesis. *Pediatr Res* 57(5 Pt 2):26R–37R.
6. Yates LL, et al. (2013) Scribble is required for normal epithelial cell-cell contacts and lumen morphogenesis in the mammalian lung. *Dev Biol* 373(2):267–280.
7. Wan H, et al. (2013) CDC42 is required for structural patterning of the lung during development. *Dev Biol* 374(1):46–57.
8. Nechiporuk T, Klezovitch O, Nguyen L, Vasioukhin V (2013) Dlg5 maintains apical aPKC and regulates progenitor differentiation during lung morphogenesis. *Dev Biol* 377(2):375–384.
9. Yates LL, Dean CH (2011) Planar polarity: A new player in both lung development and disease. *Organogenesis* 7(3):209–216.
10. Yates LL, et al. (2010) The PCP genes Celsr1 and Vangl2 are required for normal lung branching morphogenesis. *Hum Mol Genet* 19(11):2251–2267.
11. Tian Y, et al. (2011) Regulation of lung endoderm progenitor cell behavior by miR302/367. *Development* 138(7):1235–1245.
12. Perl A-KT, Wert SE, Nagy A, Lobe CG, Whitsett JA (2002) Early restriction of peripheral and proximal cell lineages during formation of the lung. *Proc Natl Acad Sci USA* 99(16):10482–10487.
13. Rawlins EL, Clark CP, Xue Y, Hogan BLM (2009) The Id2+ distal tip lung epithelium contains individual multipotent embryonic progenitor cells. *Development* 136(22):3741–3745.
14. Okubo T, Knoepfler PS, Eisenman RN, Hogan BL (2005) Nmyc plays an essential role during lung development as a dosage-sensitive regulator of progenitor cell proliferation and differentiation. *Development* 132(6):1363–1374.
15. Perl AK, Kist R, Shan Z, Scherer G, Whitsett JA. (2005) Normal lung development and function afterSox9 inactivation in the respiratory epithelium. *Genesis* 41(1):23–32.
16. Herriges JC, et al. (2012) Genome-scale study of transcription factor expression in the branching mouse lung. *Dev Dyn* 241(9):1432–1453.
17. Rawlins EL, Ostrowski LE, Randell SH, Hogan BLM (2007) Lung development and repair: Contribution of the ciliated lineage. *Proc Natl Acad Sci USA* 104(2):410–417.

18. Pritchett J, Athwal V, Roberts N, Hanley NA, Hanley KP (2011) Understanding the role of SOX9 in acquired diseases: Lessons from development. *Trends Mol Med* 17(3):166–174.
19. Jakobsen LP, et al. (2007) Pierre Robin sequence may be caused by dysregulation of SOX9 and KCNJ2. *J Med Genet* 44(6):381–386.
20. Herman TE, Siegel MJ (2012) Acampomelic campomelic dysplasia in genetic male without sex reversal. *J Perinatol* 32(1):75–77.
21. Mansour S, Hall CM, Pembrey ME, Young ID (1995) A clinical and genetic study of campomelic dysplasia. *J Med Genet* 32(6):415–420.
22. Kwok C, et al. (1995) Mutations in SOX9, the gene responsible for Campomelic dysplasia and autosomal sex reversal. *Am J Hum Genet* 57(5):1028–1036.
23. Sock E, et al. (2003) Loss of DNA-dependent dimerization of the transcription factor SOX9 as a cause for campomelic dysplasia. *Hum Mol Genet* 12(12):1439–1447.
24. Shinwell ES, Hengerer AS, Kendig JW (1988) A third case of bronchoscopic diagnosis of tracheobronchomalacia in campomelic dysplasia. *Pediatr Pulmonol* 4(3):192.
25. Houston CS, et al. (1983) The campomelic syndrome: Review, report of 17 cases, and follow-up on the currently 17-year-old boy first reported by Maroteaux et al in 1971. *Am J Med Genet* 15(1):3–28.
26. Seymour PA, et al. (2008) A dosage-dependent requirement for Sox9 in pancreatic endocrine cell formation. *Dev Biol* 323(1):19–30.
27. Seymour PA, et al. (2007) SOX9 is required for maintenance of the pancreatic progenitor cell pool. *Proc Natl Acad Sci USA* 104(6):1865–1870.
28. Lynn FC, et al. (2007) Sox9 coordinates a transcriptional network in pancreatic progenitor cells. *Proc Natl Acad Sci USA* 104(25):10500–10505.
29. Mori-Akiyama Y, et al. (2007) SOX9 is required for the differentiation of paneth cells in the intestinal epithelium. *Gastroenterology* 133(2):539–546.
30. Akiyama H (2008) Control of chondrogenesis by the transcription factor Sox9. *Mod Rheumatol* 18(3):213–219.
31. Lefebvre V, Dumitriu B, Penzo-Méndez A, Han Y, Pallavi B (2007) Control of cell fate and differentiation by Sry-related high-mobility-group box (Sox) transcription factors. *Int J Biochem Cell Biol* 39(12):2195–2214.
32. Liu C-J, et al. (2007) Transcriptional activation of cartilage oligomeric matrix protein by Sox9, Sox5, and Sox6 transcription factors and CBP/p300 coactivators. *Front Biosci* 12:3899–3910.
33. Bastide P, et al. (2007) Sox9 regulates cell proliferation and is required for Paneth cell differentiation in the intestinal epithelium. *J Cell Biol* 178(4):635–648.
34. Blache P, et al. (2004) SOX9 is an intestine crypt transcription factor, is regulated by the Wnt pathway, and represses the CDX2 and MUC2 genes. *J Cell Biol* 166(1):37–47.
35. Kist R, Schrewe H, Balling R, Scherer G (2002) Conditional inactivation of Sox9: A mouse model for campomelic dysplasia. *Genesis* 32(2):121–123.
36. Harfe BD, et al. (2004) Evidence for an expansion-based temporal Shh gradient in specifying vertebrate digit identities. *Cell* 118(4):517–528.
37. Harris KS, Zhang Z, McManus MT, Harfe BD, Sun X (2006) Dicer function is essential for lung epithelium morphogenesis. *Proc Natl Acad Sci USA* 103(7):2208–2213.
38. Schnatwinkel C, Niswander L (2013) Multiparametric image analysis of lung-branching morphogenesis. *Dev Dyn* 242(6):622–637.
39. Weaver M, Batts L, Hogan BLM (2003) Tissue interactions pattern the mesenchyme of the embryonic mouse lung. *Dev Biol* 258(1):169–184.
40. Weaver M, Dunn NR, Hogan BL (2000) Bmp4 and Fgf10 play opposing roles during lung bud morphogenesis. *Development* 127(12):2695–2704.
41. Barkauskas CE, et al. (2013) Type 2 alveolar cells are stem cells in adult lung. *J Clin Invest* 123(7):3025–3036.
42. Weaver TE, Whitsett JA (1989) Processing of hydrophobic pulmonary surfactant protein B in rat type II cells. *Am J Physiol* 257(2 Pt 1):L100–L108.
43. Glasser SW, et al. (1987) cDNA and deduced amino acid sequence of human pulmonary surfactant-associated proteolipid SPL(Phe). *Proc Natl Acad Sci USA* 84(12):4007–4011.
44. Elluru RG, Whitsett JA (2004) Potential role of Sox9 in patterning tracheal cartilage ring formation in an embryonic mouse model. *Arch Otolaryngol Head Neck Surg* 130(6):732–736.
45. Gong S, et al. (2003) A gene expression atlas of the central nervous system based on bacterial artificial chromosomes. *Nature* 425(6961):917–925.
46. Moore KA, et al. (2005) Control of basement membrane remodeling and epithelial branching morphogenesis in embryonic lung by Rho and cytoskeletal tension. *Dev Dyn* 232(2):268–281.
47. Moore KA, Huang S, Kong Y, Sunday ME, Ingber DE (2002) Control of embryonic lung branching morphogenesis by the Rho activator, cytotoxic necrotizing factor 1. *J Surg Res* 104(2):95–100.
48. Ganguly A, Yang H, Sharma R, Patel KD, Cabral F (2012) The role of microtubules and their dynamics in cell migration. *J Biol Chem* 287(52):43359–43369.
49. Ridley AJ, et al. (2003) Cell migration: Integrating signals from front to back. *Science* 302(5651):1704–1709.
50. Kuure S, et al. (2010) Actin depolymerizing factors cofilin1 and destrin are required for ureteric bud branching morphogenesis. *PLoS Genet* 6(10):e1001176.
51. Zhong Z, Baker JJ, Zylstra-Diegel CR, Williams BO (2012) Lrp5 and Lrp6 play compensatory roles in mouse intestinal development. *J Cell Biochem* 113(1):31–38.
52. Joeng KS, Schumacher CA, Zylstra-Diegel CR, Long F, Williams BO (2011) Lrp5 and Lrp6 redundantly control skeletal development in the mouse embryo. *Dev Biol* 359(2):222–229.
53. Metzger DE, Stahlman MT, Shannon JM (2008) Misexpression of ELF5 disrupts lung branching and inhibits epithelial differentiation. *Dev Biol* 320(1):149–160.
54. Yin Y, Wang F, Ornitz DM (2011) Mesothelial- and epithelial-derived FGF9 have distinct functions in the regulation of lung development. *Development* 138(15):3169–3177.
55. Rajagopal J, et al. (2008) Wnt7b stimulates embryonic lung growth by coordinately increasing the replication of epithelium and mesenchyme. *Development* 135(9):1625–1634.
56. Goss AM, et al. (2009) Wnt2/2b and β-catenin signaling are necessary and sufficient to specify lung progenitors in the foregut. *Dev Cell* 17(2):290–298.
57. Schnatwinkel C, Niswander L (2012) Nubp1 is required for lung branching morphogenesis and distal progenitor cell survival in mice. *PLoS ONE* 7(9):e44871.
58. Abler LL, Mansour SL, Sun X (2009) Conditional gene inactivation reveals roles for Fgf10 and Fgfr2 in establishing a normal pattern of epithelial branching in the mouse lung. *Dev Dyn* 238(8):1999–2013.
59. El-Hashash AHK, et al. (2011) Six1 transcription factor is critical for coordination of epithelial, mesenchymal and vascular morphogenesis in the mammalian lung. *Dev Biol* 353(2):242–258.
60. Lincoln J, Kist R, Scherer G, Yutzey KE (2007) Sox9 is required for precursor cell expansion and extracellular matrix organization during mouse heart valve development. *Dev Biol* 305(1):120–132.
61. Georg I, Barrionuevo F, Wiech T, Scherer G (2012) Sox9 and Sox8 are required for basal lamina integrity of testis cords and for suppression of FOXL2 during embryonic testis development in mice. *Biol Reprod* 87(4):99.
62. Nakamura S, et al. (2012) Analysis of medaka sox9 orthologue reveals a conserved role in germ cell maintenance. *PLoS ONE* 7(1):e29982.
63. Naitoh M, et al. (2005) Gene expression in human keloids is altered from dermal to chondrocytic and osteogenic lineage. *Genes Cells* 10(11):1081–1091.
64. Hanley KP, et al. (2008) Ectopic SOX9 mediates extracellular matrix deposition characteristic of organ fibrosis. *J Biol Chem* 283(20):14063–14071.
65. Bennett MR, et al. (2007) Laser capture microdissection-microarray analysis of focal segmental glomerulosclerosis glomeruli. *Nephron, Exp Nephrol* 107(1):e30–e40.
66. Sumi E, et al. (2007) SRY-related HMG box 9 regulates the expression of Col4a2 through transactivating its enhancer element in mesangial cells. *Am J Pathol* 170(6):1854–1864.
67. Airik R, et al. (2010) Hydroureternephrosis due to loss of Sox9-regulated smooth muscle cell differentiation of the ureteric mesenchyme. *Hum Mol Genet* 19(24):4918–4929.
68. Schulick AH, et al. (1998) Overexpression of transforming growth factor β1 in arterial endothelium causes hyperplasia, apoptosis, and cartilaginous metaplasia. *Proc Natl Acad Sci U S A* 95(12):6983–6988.
69. Oh C-D, et al. (2010) Identification of SOX9 interaction sites in the genome of chondrocytes. *PLoS ONE* 5(4):e10113.
70. Hay ED (1982) Interaction of embryonic surface and cytoskeleton with extracellular matrix. *Am J Anat* 165(1):1–12.
71. Nishizaka T, Shi Q, Sheetz MP (2000) Position-dependent linkages of fibronectin-integrin-cytoskeleton. *Proc Natl Acad Sci USA* 97(2):692–697.
72. Hotta A, et al. (2010) Laminin-based cell adhesion anchors microtubule plus ends to the epithelial cell basal cortex through LL5alpha/beta. *J Cell Biol* 189(5):901–917.
73. Betters E, Liu Y, Kjaeldgaard A, Sundström E, García-Castro MI (2010) Analysis of early human neural crest development. *Dev Biol* 344(2):578–592.
74. Chakravarty G, et al. (2011) Prognostic significance of cytoplasmic SOX9 in invasive ductal carcinoma and metastatic breast cancer. *Exp Biol Med (Maywood)* 236(2):145–155.
75. Bowen KA, et al. (2009) PTEN loss induces epithelial—mesenchymal transition in human colon cancer cells. *Anticancer Res* 29(11):4439–4449.
76. Wang H, et al. (2008) SOX9 is expressed in human fetal prostate epithelium and enhances prostate cancer invasion. *Cancer Res* 68(6):1625–1630.
77. Rao P, Fuller GN, Prieto VG (2010) Expression of Sox-9 in metastatic melanoma—a potential diagnostic pitfall. *Am J Dermatopathol* 32(3):262–266.
78. Seymour PA, et al. (2012) A Sox9/Fgf feed-forward loop maintains pancreatic organ identity. *Development* 139(18):3363–3372.
79. Furuyama K, et al. (2011) Continuous cell supply from a Sox9-expressing progenitor zone in adult liver, exocrine pancreas and intestine. *Nat Genet* 43(1):34–41.
80. Kopp JL, et al. (2011) Sox9+ ductal cells are multipotent progenitors throughout development but do not produce new endocrine cells in the normal or injured adult pancreas. *Development* 138(4):653–665.
81. Brault V, et al. (2001) Inactivation of the beta-catenin gene by Wnt1-Cre-mediated deletion results in dramatic brain malformation and failure of craniofacial development. *Development* 128(8):1253–1264.
82. Belteki G, et al. (2005) Conditional and inducible transgene expression in mice through the combinatorial use of Cre-mediated recombination and tetracycline induction. *Nucleic Acids Res* 33(5):e51.
83. Del Moral P-M, Warburton D (2010) Explant culture of mouse embryonic whole lung, isolated epithelium, or mesenchyme under chemically defined conditions as a system to evaluate the molecular mechanism of branching morphogenesis and cellular differentiation. *Methods Mol Biol* 633:71–79.
84. Spence JR, et al. (2011) Directed differentiation of human pluripotent stem cells into intestinal tissue in vitro. *Nature* 470(7332):105–109.
85. Spence JR, et al. (2009) Sox17 regulates organ lineage segregation of ventral foregut progenitor cells. *Dev Cell* 17(1):62–74.
86. Di Giacomo G, et al. (2006) Spatio-temporal expression of Pbx3 during mouse organogenesis. *Gene Expr Patterns* 6(7):747–757.
87. Mendelsohn C, Batourina E, Fung S, Gilbert T, Dodd J (1999) Stromal cells mediate retinoid-dependent functions essential for renal development. *Development* 126(6):1139–1148.
88. Jones CM, Lyons KM, Hogan BL (1991) Involvement of Bone Morphogenetic Protein-4 (BMP-4) and Vgr-1 in morphogenesis and neurogenesis in the mouse. *Development* 111(2):531–542.
89. Li X, et al. (2009) Dynamic patterning at the pylorus: Formation of an epithelial intestine-stomach boundary in late fetal life. *Dev Dyn* 238(12):3205–3217.
90. Echelard Y, et al. (1993) Sonic hedgehog, a member of a family of putative signaling molecules, is implicated in the regulation of CNS polarity. *Cell* 75(7):1417–1430.
91. Prasov L, Nagy M, Rudolph DD, Glaser T (2012) Math5 (Atoh7) gene dosage limits retinal ganglion cell genesis. *Neuroreport* 23(10):631–634.